*J. Chem. Sci.* Vol. 127, No. 4, April 2015, pp. 649–661. 
DOI 10.1007/s12039-015-0817-y

# Synthesis and bio-catalytic activity of isostructural cobalt(III)-phenanthroline complexes

DHANANJAY DEY[a], ARNAB BASU ROY[a], ANANDAN RANJANI[b], LOGANATHAN GAYATHRI[b], SARAVANAN CHANDRALEKA[b,§], DHARUMADURAI DHANASEKARAN[b], MOHAMMAD ABDULKADER AKBARSHA[c], CHUNG-YU SHEN[d], HUI-LIEN TSAI[d], MILAN MAJI[e], NIRANJAN KOLE[a] and BHASKAR BISWAS[a,*]

[a]Department of Chemistry, Raghunathpur College, Purulia 723133, India
[b]Department of Microbiology, Bharathidasan University, Tiruchirappalli 620 024, India
[c]Mahatma Gandhi-Doerenkamp Centre, Bharathidasan University, Tiruchirappalli 620 024, India
[d]Department of Chemistry, National Cheng Kung University, Tainan City, 70101, Taiwan
[e]Department of Chemistry, National Institute of Technology, Mahatma Gandhi Avenue, Durgapur 713209, India
[§]*Present address*: Department of Chemistry, Urumu Dhanalakshmi College, Tiruchirappalli 620019, India
e-mail: mr.bbiswas@rediffmail.com; icbbiswas@gmail.com

MS received 02 July 2014; revised 06 November 2014; accepted 10 November 2014

**Abstract.** We have synthesized two isostructural mononuclear cobalt(III) complexes $[\mathbf{1}]NO_3{\cdot}3H_2O$ and $[\mathbf{1}]NO_3{\cdot}CH_3CO_2H{\cdot}H_2O$ $\{[\mathbf{1}]^+ = [Co(1,10\text{-phenanthroline})_2Cl_2]^+\}$ and characterized by single crystal X-ray structural analyses. Mass spectral studies of the complexes indicate both the compounds to produce identical cationic species viz., $[Co(phen)_2Cl_2]^+$ in methanol solution. $[\mathbf{1}]^+$ has been evaluated as model system for the catechol oxidase enzyme by using *3,5-di*-tert-butylcatechol (3,5-DTBC) as the substrate in methanol medium, which revealed that the cationic complex efficiently inhibits catalytic activity with $k_{cat}$ value $9.65\times10^2$ $h^{-1}$. $[\mathbf{1}]^+$ cleaved pBR 322 DNA without addition of an activating agent. Further, the anti-cancer activity of $[\mathbf{1}]^+$ on human hepatocarcinoma cell line (HepG2) has been examined. The induction of apoptosis induced in the cell line was assessed base on the changes in cell morphology, which showed the efficacy of $[\mathbf{1}]^+$ to induce apoptosis in 53% of cells during 24 h treatment. Interestingly, the observed $IC_{50}$ values reveal that $[\mathbf{1}]^+$ brings about conformational change on DNA strongly and exhibits remarkable cytotoxicity.

**Keywords.** Cobalt(III); X-ray structure; Catecholase activity; DNA cleavage; Anti-cancer activity.

## 1. Introduction

Cobalt(III) compounds of polycyclic heteroaromatics with transition metals form a class of DNA interacting substances that have received considerable attention over the years, as they combine properties of traditional DNA interacting polycyclic aromatics with important photophysical and photochemical potentials offered by the metal into rigid structures spanning all three dimensions.[1–3] The design of small cationic molecules that react at specific sequences of DNA under physiological conditions via oxidative and hydrolytic cleavage has been attracting great interest in the field of bioinorganic chemistry. The application of octahedral complexes has allowed the targeting of specific DNA sites by matching the shape, symmetry and functionality of the metal complex to those of the DNA target.[4] Due to the unusual binding properties and general photo-activity, these coordination compounds are candidates available as DNA secondary structure probes, photocleavers and anti-tumour drugs.[5–8]

The oxidation of organic compounds is an important and widely used reaction in laboratory scale organic synthesis as well as in large scale chemical industry.[9–11] An ideal oxidant for any large scale oxidation reaction should be easily accessible, cheap and non-toxic like dioxygen.[12–14] It is easily available since it is present in air and the only by-product produced from its decomposition is water. In this respect, the oxidation of a wide range of *o*-diphenols (catechols), such as caffeic acid, to the corresponding quinones using molecular oxygen as oxidant and a copper enzyme Catechol Oxidase ($CO_x$), as catalyst has received considerable attraction to reveal mechanistic aspect, catalytic activity, product formation

*For correspondence

selectivity, structure-reactivity relationship and so on.[15–17] The quinines which are highly reactive compounds undergo auto-polymerization leading to the formation of a brown polyphenolic pigment, *i.e.* melanin, a process thought to protect a damaged tissue against pathogens or insects.[18] Though cobalt complexes have been regarded as very efficient and selective catalysts towards different organic transformations, cobalt(III)-phenanthroline complexes as biomimetic models of catechol oxidase have not been extensively studied.[19–21]

Herein, we report two new isostructural mononuclear cobalt(III)-phenanthroline complexes containing hetero anions and solvate molecules in Co(III)–1,10-phenanthroline crystalline host at room temperature. We have investigated the catalytic activity of $[\mathbf{1}]^+$, $\{[\mathbf{1}]^+ = [Co(1,10\text{-phenanthroline})_2Cl_2]^+\}$, towards *3,5-di*-tert-butylcatechol as bio-mimetic model for catecholase oxidase in methanolic medium. Since detailed investigation of DNA binding and DNA photocleavage studies for *cis*-dichlorobis(diimine)cobalt(III)chloride complexes was performed by Joshi *et al* in 2006,[22] we have explored the cleavage efficiency on pBR 322 DNA without adding any external agents. Also, $[1]^+$ proved to be an efficient cytotoxic agent against human hepatocellular carcinoma cell line HepG2.

## 2. Experimental

### 2.1 *Preparation of the complexes*

2.1a *Chemicals, solvents and starting materials*: High purity 1,10-phenanthroline (Lancaster, UK), ammonium ceric nitrate (Aldrich, UK), cobalt(II) chloride hexahydrate (E. Merck, India), and glacial acetic acid (E. Merck, India) were purchased and used as received. All the other reagents and solvents are of Analytical grade (A.R. grade) and were purchased from commercial sources and used as received.

2.1b *General synthesis of compounds*: Cobalt(III) complexes were synthesized by mixing phen (0.198 g, 1 mmol), $CoCl_2.6H_2O$ (0.237 g, 1 mmol) and ceric ammonium nitrate in 1:1:2 ratio. For the synthesis of $[\mathbf{1}]NO_3{\cdot}3H_2O$, 4/6 (v/v) AcOH:$H_2O$ (7N) has been used as solvent mixture, whereas for $[\mathbf{1}]NO_3{\cdot}CH_3CO_2H{\cdot}H_2O$, we used 7/3 (v/v) AcOH:$H_2O$ (12N). The reaction mixture was kept on magnetic stirrer for another 30 mins. The dark brown supernatant liquids were kept in air for slow evaporation. After 15–20 days the fine microcrystalline compounds were separated out, washed in hexane and dried *in vacuo* over silica gel indicator. The spectroscopic measurements and elemental analyses confirm the structural formation of the complexes. Yield of $[\mathbf{1}]NO_3{\cdot}3H_2O$ (based on metal salt): 0.3180 g (73.1%). Anal cal. for $C_{24}H_{22}N_5Cl_2O_6Co$ : C, 47.54; H, 3.66; N, 11.55; Found: C, 47.45; H, 3.58; N, 11.59. Selected IR bands (KBr pellet, $cm^{-1}$): 3417 (s), 1384 (s), 1426 (m), 1604 (s). UV-Vis (λ,nm): 232, 265, 450–650 (broad band). Yield of $[\mathbf{1}]NO_3{\cdot}CH_3CO_2H{\cdot}H_2O$ (based on metal salt): 0.3060 g (70.3%). Anal cal. for $C_{26}H_{22}N_5Cl_2O_6Co$: C, 49.54; H, 3.52; N, 11.11; Found: C, 49.43; H, 3.43; N, 11.18. Selected IR bands (KBr pellet, $cm^{-1}$): 3401 (s), 1383 (s), 1424 (m), 1609 (s). UV-Vis (λ, nm): 233, 267, 450–650 (broad band).

### 2.2 *Physical measurements*

Infrared spectra (KBr) were recorded with a FTIR-8400S SHIMADZU spectrophotometer in the range 400–3600 $cm^{-1}$. $^1H$ NMR spectra in DMSO-$d_6$ were obtained on a Bruker Avance 300 MHz spectrometer at 25°C and was recorded at 299.948 MHz. Chemical shifts are reported with reference to $SiMe_4$. Diffuse reflectance spectra were obtained with a Varian Cary 5E spectrometer using polytetrafluoroethylene (PTFE) as a reference. Ground state absorption was measured with a JASCO V-530 UV-vis spectrophotometer. Thermal analyses of the compounds were carried out on a PerkinElmer Diamond TG/DTA system up to 700°C in a static nitrogen atmosphere with a heating rate of 10°C/min. Elemental analyses were performed on a Perkin Elmer 2400 CHN microanalyser. Electrospray ionization (ESI) mass spectrum was recorded using a Q-tof-micro-quadruple mass spectrometer.

### 2.3 *X-ray diffraction study*

Single crystal data of $[\mathbf{1}]NO_3{\cdot}3H_2O$ and $[\mathbf{1}]NO_3{\cdot}CH_3CO_2H{\cdot}H_2O$ were collected on a Bruker SMART APEX II CCD diffractometer using Mo-$K_\alpha$ radiation ($\lambda$ = 0.71073 Å) at 220 and 150 K respectively. Systematic absent reflections led to the identification of identical space group Cc (9) for $[\mathbf{1}]NO_3{\cdot}3H_2O$ and $[\mathbf{1}]NO_3{\cdot}CH_3CO_2H{\cdot}H_2O$ crystals. Of the 9452 and 6018 total reflections for the two respective complexes 4708 and 2421 with $I>2\sigma$ were used for structure solutions. The structures were solved by direct methods, and the structure solution and refinement were based on $|F|^2$. All non-hydrogen atoms were refined with anisotropic displacement parameters whereas hydrogen atoms were placed in calculated positions when possible and given isotropic U values 1.2 times that of the atom to which they are bonded. Fourier map showed the maximum and minimum peak heights at 0.40, −0.35 for $[\mathbf{1}]NO_3{\cdot}3H_2O$

and 0.25 and −0.26 for [**1**]$NO_3 \cdot CH_3CO_2H \cdot H_2O$ with no chemical significance. All calculations were carried out using Bruker programs[23] and SHELXL−97.[24]

### 2.4 *Catalytic oxidation of 3,5-DTBC*

In order to examine the catecholase activity of the complex, a $10^{-4}$M solution of $[\mathbf{1}]^+$ in methanol solvent was treated with 100 equiv. of *3,5-di*tert-butylcatechol (3,5-DTBC) under aerobic conditions at room temperature. Absorbance *vs.* wavelength (wavelength scans) of the solution was recorded at a regular time intervals of 5 min in the wavelength range 300–500 nm for up to 60 min. It may be noted here that a blank experiment without catalyst does not show formation of the quinone up to 6 h in MeOH.

To determine the dependence of rate on substrate concentration and various kinetic parameters, a $10^{-4}$M solution of the complex was treated with at least 10 equiv. of substrate to maintain the pseudo- first order condition. The reaction was followed spectrophotometrically by monitoring the increase in the absorbance at 398 nm (Quinone band maxima) as a function of time (time scan) up to 60 min.

### 2.5 *DNA cleavage studies*

Cleavage of pBR 322 DNA by $[\mathbf{1}]^+$ was monitored by agarose gel electrophoresis technique. The complex (25, 50, 75 and 100 $\mu$g) solutions were incubated with plasmid DNA for an hour at 37°C. After incubation 2 $\mu$ l of bromophenol blue dye was mixed with $[\mathbf{1}]^+$ and loaded carefully into the electrophoresis chamber wells along with the control DNA. TAE buffer was used as a running buffer and $[\mathbf{1}]^+$ is stable in this buffer medium. The plasmid DNA, thus treated, was loaded on agarose gel and constant 50 V was applied for 30 min. Then the bands were stained with EB and observed in the gel documentation system and photographed to determine the extent of DNA cleavage and the results are compared with the control.

To confirm the cleavage activity of the $[\mathbf{1}]^+$, UV spectroscopic analysis was performed. 1 $\mu$L of the DNA was diluted with 50 $\mu$L of TE buffer and absorbance was read at 260 nm for the control DNA, along with the test samples containing different concentrations of $[\mathbf{1}]^+$ and the DNA. The concentration of the DNA was calculated using the formula:

DNA concentration ($\mu$g/mL) = (OD 260) × (dilution factor) × (50 $\mu$g DNA/mL)/(OD260 unit)

### 2.6 *Anti-cancer activity of the [1]$^+$ complex*

2.6a *Cell culture*: The human hepatocarcinoma (HepG2) cell line was obtained from the National Centre for Cell Science (NCCS), Pune, India. The cells were cultured in DMEM medium (Sigma–Aldrich, St. Louis, MO, USA), supplemented with 10% fetal bovine serum (Gibco) and 100 U/mL of penicillin and 100 $\mu$g/mL of streptomycin as antibiotics (Gibco), in 96 well culture plates, at 37°C, in a humidified atmosphere of 5% $CO_2$, in a $CO_2$ incubator (Forma, Thermo Scientific, USA). All experiments were performed using cells from passage 15 or less.

2.6b *Cytotoxicity assay (MTT assay)*: The Co(III) complex, $[1]^+$ in the concentration range 50–500 $\mu$M was dissolved in DMSO and $[1]^+$ is stable in this medium. It was added to the wells 24 h after seeding of $5 \times 10^3$ cells per well in 200 $\mu$L of fresh culture medium. DMSO solution was used as the solvent control. A miniaturized viability assay using 3-(4,5-dimethylthiazol-2-yl)-2,5-diphenyl-tetrazolium bromide (MTT) was carried out according to the method described by Mosmann.[25] After 24 and 48 h, 20 $\mu$L of MTT solution [5 mg/mL in phosphate-buffered saline (PBS)] was added to each well and the plates were wrapped with aluminum foil and incubated for 4 h at 37°C. The purple formazan product was dissolved by addition of 100 $\mu$L of DMSO to each well. The absorbance was monitored at 570 nm (measurement) and 630 nm (reference) using a 96-well plate reader (Bio-Rad, Hercules, CA, USA). Data were collected for three replicates each and used to calculate the mean. The percentage inhibition was calculated, from this data, using the formula:

$$= \frac{\text{Mean OD of untreated cells (control) - Mean OD of treated cells}(treat) \times 100}{\text{Mean absorbance of untreated cells (control)}}$$

From these data, the $IC_{50}$ (the concentration at which $[\mathbf{1}]^+$ killed 50% of the cells at the respective durations of treatment) for 24 and 48 h treatment were arrived at.

2.6c *Acridine orange (AO) and ethidium bromide (EB) staining*: Acridine orange and ethidium bromide staining was performed as described by Spector *et al.*[26] The cell suspension of each sample containing $5 \times 10^5$ cells, was treated with 25 $\mu$L of AO and EB solution (3.8 $\mu$M of AO and 2.5 $\mu$M of EB in PBS) and examined in a fluorescent microscope (Carl Zeiss, Germany) using an UV filter (450–490 nm). Three hundred cells per sample were counted in triplicate for each dose point. The cells were scored as viable, apoptotic or necrotic as judged by the staining, nuclear morphology and membrane integrity[26] and the percentages of apoptotic and necrotic cells were then calculated. Morphological changes were also observed and photographed.

2.6d *Hoechst 33528 Staining*: The Human Hepatocarcinoma (HepG@) cells were cultured in 6-well plates and treated with $IC_{50}$ concentration of $[\mathbf{1}]^+$. After 24 h incubation, the treated and untreated cells were harvested and stained with Hoechst 33258 (1 mg/mL, aqueous) for 5 min at room temperature. A drop of cell suspension was placed on a glass slide, and a cover slip was laid over to reduce light diffraction. At random 300 cells, in duplicate, were observed at ×400 in a fluorescent microscope (Carl Zeiss, Jena, Germany) fitted with a 377–355 nm filter, and the percentage of cells reflecting pathological changes was calculated.

### 2.7 *Thermogravimetric analysis*

The thermal behaviour of the complexes $[\mathbf{1}]NO_3{\cdot}3H_2O$ and $[\mathbf{1}]NO_3{\cdot}CH_3CO_2H{\cdot}H_2O$ were followed up to 700°C in a static nitrogen atmosphere with a heating rate of 10°C per minute.

## 3. Results and Discussion

### 3.1 *Syntheses and formulation*

The mononuclear cobalt(III) complexes, $[\mathbf{1}]NO_3{\cdot}3H_2O$ and $[\mathbf{1}]NO_3{\cdot}CH_3CO_2H{\cdot}H_2O$ were prepared by addition of 1,10-phenanthroline to a solution of $CoCl_2{\cdot}6H_2O$ followed by the addition of solid CAN in aqueous acetic acid solution (v/v) at different pH for both complexes at room temperature, respectively. Interestingly, different composition of solvent mixture produces different solvate molecules with identical Co(III)-coordination linkages. The schematic presentation of syntheses is given below (Scheme 1):

### 3.2 *Spectroscopic characterization and solution properties*

Two isostructural Co(III) complexes, $[Co(phen)_2Cl_2]NO_3{\cdot}3H_2O$ and $[Co(phen)_2Cl_2]NO_3{\cdot}CH_3CO_2H{\cdot}H_2O$ were prepared by addition of 1,10-phen to a solution of $CoCl_2{\cdot}6H_2O$ followed by the addition of solid CAN in aqueous acetic acid solutions having two different acetic acid concentrations. However, such compounds could not be prepared in other mixed aqueous solvents like methanol-water, acetonitrile-water, dichloromethane-water or in pure solvents like water and methanol. Here, CAN is used to oxidize the metal ion at +3 oxidation level and it also supplies heavier nitrate anion to stabilize the complexes. The $[Co(phen)_2Cl_2]^+$ is soluble in all the common solvents like methanol, acetonitrile, water, etc.

The IR spectra of $[\mathbf{1}]NO_3{\cdot}3H_2O$ and $[\mathbf{1}]NO_3{\cdot}CH_3CO_2H{\cdot}H_2O$ contain characteristic strong bands for the $NO_3^-$ anion at ~1384 $cm^{-1}$. These bands are overlapped with a set of bands for the 1,10-phen fragment, which, in turn, also shows bands at about 1000 and 3100 $cm^{-1}$.[27] Bands characteristic for the $\alpha$-diimine ligands are clearly observed at ~1600 $cm^{-1}$. Water molecules in the structure of the complexes were detected in the IR spectra by a broad band centred at about 3401 and 3417 $cm^{-1}$.

The diffuse reflectance spectra of the cobalt(III) complexes exhibit three regions: three absorption bands in the UV region, corresponding to the intra-ligand and ligand-to-metal transitions of 1,10-phen, a second range from about 450 to 650 nm and a third weak band centred at about 800 nm (figure S1). The latter two bands originate from the same $d - d$ transitions.[28]

NMR spectroscopy experiments on $[\mathbf{1}]NO_3{\cdot}3H_2O$ and $[\mathbf{1}]NO_3{\cdot}CH_3CO_2H{\cdot}H_2O$ testify to its diamagnetic nature. The $^1H$ NMR spectra of the complexes contain four doublet peaks at ~10.03, 9.31, 8.82 and 8.38 ppm, and two triplet peaks at ~8.5 and 7.6 ppm (figure S2) for the 1,10-phenanthroline ligands with characteristic coupling constants $^3J_{H,H} = 7.66$–$7.53$ Hz.

In order to probe the solution stability of the complexes, we have performed UV–Vis spectral measurements for methanolic solution of $[\mathbf{1}]NO_3{\cdot}3H_2O$ and $[\mathbf{1}]NO_3{\cdot}CH_3CO_2H{\cdot}H_2O$ at room temperature and both the compounds produced almost identical band at ~232, 267, 341 and 540 nm. Low intensity and broad transitions at 540 nm are attributed to ligand field bands in $Co^{III}$ octahedral field (figure S3) and these bands remained unaffected over a period of at least 5 days revealing that the complexes are stable in solution at room temperature. Mass spectral analysis of the cobalt complexes further consolidates this fact by producing molecular ion peak at m/z 489.0263 (Calc. 489.0084) (figure S4) in methanol and this experimental peak corresponds to the existence of the stable cationic species as $[Co(1,10\text{-phen})_2Cl_2]^+$ in solution.

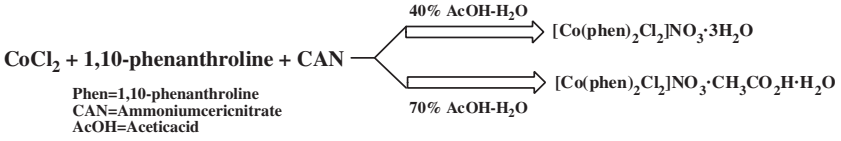


**Scheme 1.** Preparation of cobalt(III) complexes.

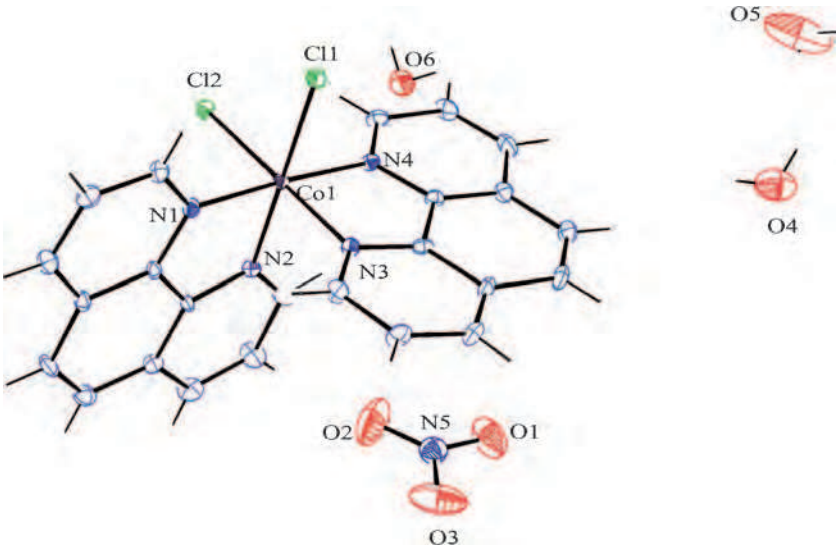


**Figure 1.** ORTEP diagram of [**1**]$NO_3 \cdot 3H_2O$ (30% ellipsoid probability) with atom numbering scheme.

### 3.3 *Description of crystal structures*

The single crystal X-ray diffraction analysis reveals that both the crystal lattices of [**1**]$NO_3 \cdot 3H_2O$ and [**1**]$NO_3 \cdot CH_3CO_2H \cdot H_2O$ consist of identical mononuclear cationic unit $[Co(phen)_2Cl_2]^+$ but differ in inclusion of solvent molecules. The ORTEP diagram with atom numbering scheme of the mononuclear complexes [**1**]$NO_3 \cdot 3H_2O$ and [**1**]$NO_3 \cdot CH_3CO_2H \cdot H_2O$ are shown in figures 1 and 2. The coordination geometry around each (III) centre is best described as distorted octahedron with a $CoN_4Cl_2$ chromophore. The coordination includes two coordinated phenanthroline ligands, along with two coordinated Cl atoms in mutual *cis* orientation in [**1**]$NO_3 \cdot 3H_2O$ and [**1**]$NO_3 \cdot CH_3CO_2H \cdot H_2O$. The angles 92.15(4)° and 91.89(3)° between the two coordinated chlorine atoms around Co(III) centre in [**1**]$NO_3 \cdot 3H_2O$ and [**1**]$NO_3 \cdot CH_3CO_2H \cdot H_2O$ as Cl(1)-Co(1)-Cl(2) indicate the *cisoid* representation of the structures. A summary of the crystallographic data and structure refinement parameters is given in table 1. The bond angle and bond distance data are given in table S1 for [**1**]$NO_3 \cdot 3H_2O$ and table S2 for [**1**]$NO_3 \cdot CH_3CO_2H \cdot H_2O$.

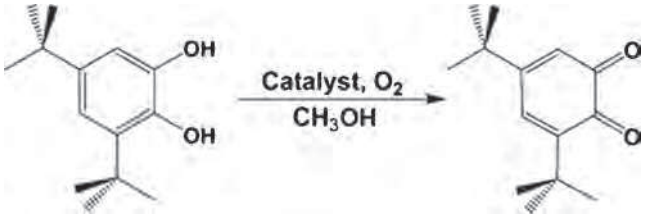


**Scheme 2.** Catalytic Oxidation of 3,5-DTBC to 3,5-DTBQ in air-saturated methanol solvent.

### 3.4 *Catecholase activity of [1]$^+$*

Catechol oxidases are type III copper proteins which catalyze the oxidation of catechols to quinones in the presence of oxygen.[29] The catecholase activity of the $[Co(phen)_2Cl_2]^+$ complex, [**1**]$^+$ was studied using 3,5-di-tert-butylcatechol (3,5-DTBC) as a convenient model substrate, in air-saturated methanol solvent at room temperature (25°C). For this purpose, a $1 \times 10^{-4}$M solution of this complex was treated with $1 \times 10^{-2}$M (100 equiv.) of 3,5-DTBC and the course of the reaction was followed by recording the UV–vis spectra of the mixture at an interval of 5 min for 1 h (Scheme 2).

Spectral bands at 232, 267, 341 and 540 nm appeared in the electronic spectrum of complex [**1**]$^+$ in methanol, whereas 3,5-DTBC showed a single band at 284 nm. As the reaction proceeded, there was a gradual decrease in intensity of the band at 284 nm due to the catechol[30] and an initial new band was formed at ~398 nm (figure 3), which indicated the formation of the respective quinone derivative and the band maximum was gradually shifted to 398 nm. 3,5-DTBQ was purified by column chromatography and isolated in high yield (76.2% for **1**) by slow evaporation of the eluant. The product was identified by $^1$H NMR spectroscopy. $^1$H NMR ($CDCl_3$, 400 MHz) $\delta_H$: 1.15 (s, 9H), 1.20 (s, 9H), 6.15 (d, $J = 2.4$ Hz, 1H), 6.86 (d, $J = 2.4$ Hz, 1H).

Kinetic studies were performed to understand the extent of the efficiency. The kinetics of oxidation of 3,5-DTBC were determined by the method of initial rates and involved monitoring the growth of the quinone band at 398 nm as a function of time.[31] For this purpose, 0.04 mL of the complex solution, with a constant concentration of $1 \times 10^{-4}$ M, was added to 2 mL of 3,5-DTBC

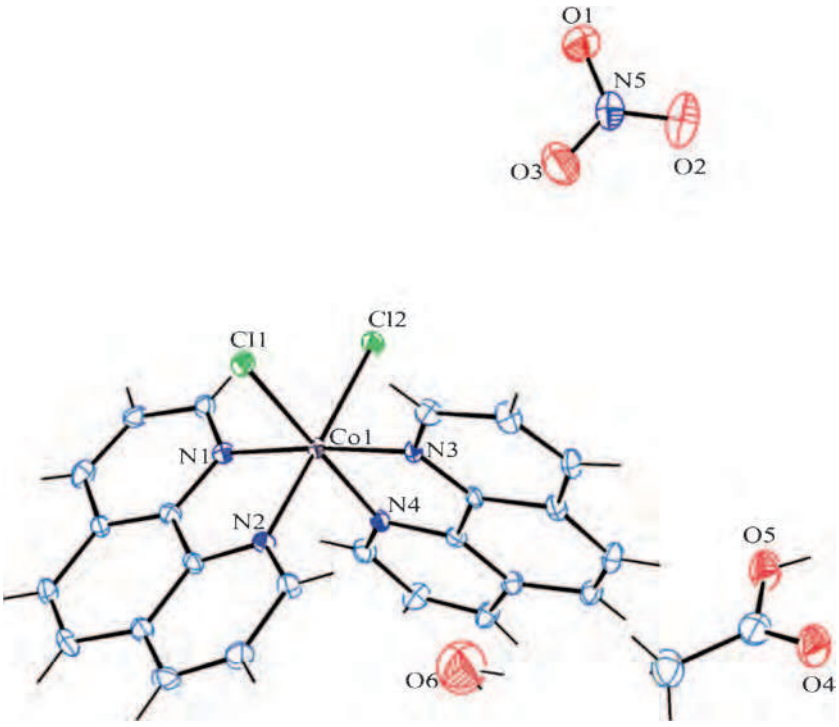


**Figure 2.** ORTEP diagram of [**1**]$NO_3 \cdot CH_3CO_2H \cdot H_2O$ (30% ellipsoid probability) with atom numbering scheme.

**Table 1.** Crystal data and structure refinement parameters for [**1**]$NO_3 \cdot 3H_2O$ and [**1**]$NO_3 \cdot CH_3CO_2H \cdot H_2O$.

| Parameters | [**1**]$NO_3 \cdot 3H_2O$ | [**1**]$NO_3 \cdot CH_3CO_2H \cdot H_2O$ |
|---|---|---|
| Empirical formula | $C_{24}H_{22}N_5Cl_2O_6Co$ | $C_{26}H_{22}N_5Cl_2O_6Co$ |
| Formula weight | 606.30 | 630.32 |
| Temperature (K) | 220(2) | 150(2) |
| Crystal system | Monoclinic | Monoclinic |
| Space group | Cc(9) | Cc(9) |
| a (Å) | 15.2063(15) | 15.3215(9) |
| b (Å) | 13.4762(13) | 13.3189(17) |
| c (Å) | 12.3354(12) | 12.8357(17) |
| Volume (Å$^3$) | 2501.5(4) | 2578.0(6) |
| Z | 4 | 4 |
| $\rho$ (gcm$^{-3}$) | 1.610 | 1.624 |
| $\mu$ (mm$^{-1}$) | 0.951 | 0.927 |
| F (000) | 1240 | 1288 |
| $\theta$ ranges (°) | 2.0-28.3 | 2.0-25.0 |
| $R_{int}$ | 0.014 | 0.016 |
| R (reflections) | 9452 | 6018 |
| wR2 (reflections) | 4708 | 2421 |
| Final R indices | 0.0280,0.0799 | 0.0293, 0.0852 |
| Largest peak and hole (eA°$^{-3}$) | 0.40,-0.35 | 0.25,-0.26 |

of a particular concentration (varying its concentration from $1 \times 10^{-3}$ M to $1 \times 10^{-2}$ M) to achieve the ultimate concentration of the complex as $1 \times 10^{-4}$ M. The colour of the solution gradually turned deep brown, indicating the gradual conversion of 3,5-DTBC to 3,5-DTBQ. The experiments were done at a constant temperature of 25°C under aerobic conditions. For a particular complex-substrate mixture, time scan at the maximum of the quinone band (398 nm) was carried out for a period of 60 min. The rate constants versus concentration of the substrate data were then analyzed on the basis of the Michaelis–Menten approach of enzymatic kinetics to get the Lineweaver–Burk plot (double reciprocal), as well as the values of the parameters $V_{max}$, $K_m$, and $K_{cat}$. The observed rate constant versus substrate concentration plot and the Lineweaver–Burk plot for complex

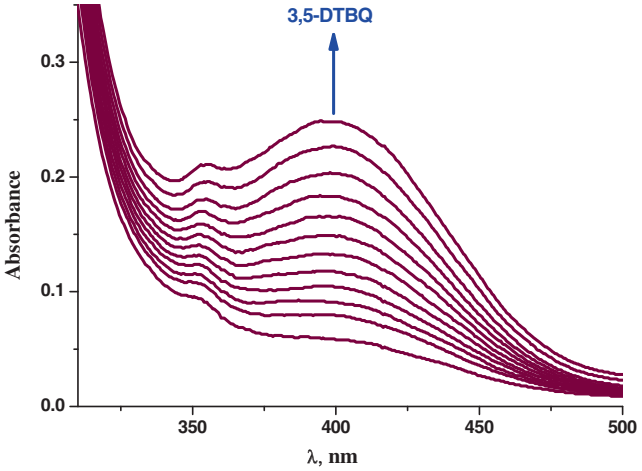


**Figure 3.** Increase of quinone band at 398 nm after addition of 100 equivalents of 3,5-DTBC to a solution containing $[\mathbf{1}]^+$ ($10^{-4}$ M) in methanol at $25^0$C. The spectra were recorded after every 5 min.

$[\mathbf{1}]^+$ in MeOH is shown in figure 4. To reveal high catalytic activity of $[\mathbf{1}]^+$, we drew a comparison between our cobalt(III) complex and some other mono- and polynuclear cobalt complexes.[32–35] The data obtained from the Lineweaver–Burk plot model were used for a comparison of catalytic activity towards the oxidation of 3,5-DTBC as shown in table 2. The kinetic parameters of $[\mathbf{1}]^+$ are also presented in table 2. This comparison also indicates that $[\mathbf{1}]^+$ acts as a better and effective catalyst towards catecholase activity than some recently reported ones.[32–35]

### 3.5 *Mechanistic aspects towards catalytic oxidation of 3,5-di-tert-butylcatechol (DTBC) by [**1**]$^+$*

Regarding complexes of metal ions of cobalt as active catalysts for catechol oxidase activity, two or three examples of mononuclear cobalt complexes are known in literature.[15b,c,33] So, cobalt(III) compound, $[\mathbf{1}]^+$ in the present investigation is one of the few examples of mononuclear cobalt complexes containing catalyst of catecholase activity for which both the single crystal X-ray structure and $K_{cat}$ value has been determined. To get an insight into the nature of possible complex–substrate intermediates, ESI-MS positive spectra of a 1:100 mixture of $[\mathbf{1}]^+$ and 3,5-DTBCH$_2$ were recorded after 20 min of mixing in methanol. The observed patterns are presented in figure S5 (Scheme 3).

Most importantly, characteristic peaks are observed at m/z = 243.55 and 641.02. The peaks at m/z = 243.55 and 641.02 correspond, respectively, to the quinone–sodium aggregate $[(3,5\text{-DTBQ})Na]^+$ and $[Co^{II}(1,10\text{-phen})_2(3,5\text{-DTBC}^{2-})H]^+$. The latter peaking at m/z = 641.02 is interesting because the peak position in the observed mass spectral pattern clearly indicates that the peak arises due to 1 : 1 complex–substrate aggregate $[Co^{II}(1,10\text{-phen})_2(3,5\text{-DTBC}^{2-})H]^+$. It is logical to consider the dianionic 3,5-DTBCH$^{2-}$ species in $[Co^{II}(1,10\text{-phen})_2(3,5\text{-DTBC}^{2-})H]^+$ as coordinated in bidentate chelating mode through the phenolate oxygen atom to the cobalt(III) centre. The intermediate Co(III) complex is reduced to Co(II) by the catechol derivative, and 3,5-DTBC itself gets oxidised to quinone in presence of oxygen with the production of water.

Whatever the aftermath, coordination of the catechol moiety to the metal centre is an essential requirement for a complex to show catecholase activity. In the two proposed mechanisms regarding the in vivo cycle, 1:1 adduct formation between a dicopper(II) core and the substrate has been mentioned. While monodentate asymmetric coordination of the substrate has been proposed in one mechanism (Krebs's mechanism),[17c,d] simultaneous coordination of the substrate to both copper centres in the dinucleating bridging is suggested in the second (Solomon's mechanism).[17b] Although our cationic mononuclear cobalt(III) complex is not a $Cu^{II}Cu^{II}$ molecular system, one 1:1 complex substrate aggregate $[Co^{II}(1,10\text{-phen})_2(3,5\text{-DTBC}^{2-})H]^+$ having a bidentate chelating catechol moiety in that aggregate has been identified in the ESI-MS positive spectrum in the present investigation. So, after comparing these data, it can be concluded that the reported cobalt(III) complex is quite an efficient catalyst and has an appreciable turnover rate in methanolic medium. Besides, $[\mathbf{1}]^+$ being a mononuclear cobalt(III) complex with non-copper centre is mimicking an enzyme with a dicopper active site.

### 3.6 *DNA cleavage studies*

The irradiation of pBR322 plasmid DNA in the presence of the $[\mathbf{1}]^+$ was studied so as to determine the efficiency with which it sensitizes DNA cleavage. This can be achieved by monitoring the transition from the naturally occurring, covalently closed circular form (Form I) to the open circular relaxed form (Form II). This occurs when one of the strands of the plasmid is nicked, and can be determined by gel electrophoresis of the plasmid. Extended irradiation results in a build up of nicks on both strands of the plasmid, which eventually results in its opening to the linear form (Form III). When circular plasmid DNA is subjected to gel electrophoresis, relatively faster migration is observed in the supercoiled form (Form I). Form (II) migrates slowly and Form III migrates between Form II and Form I.[36,37]

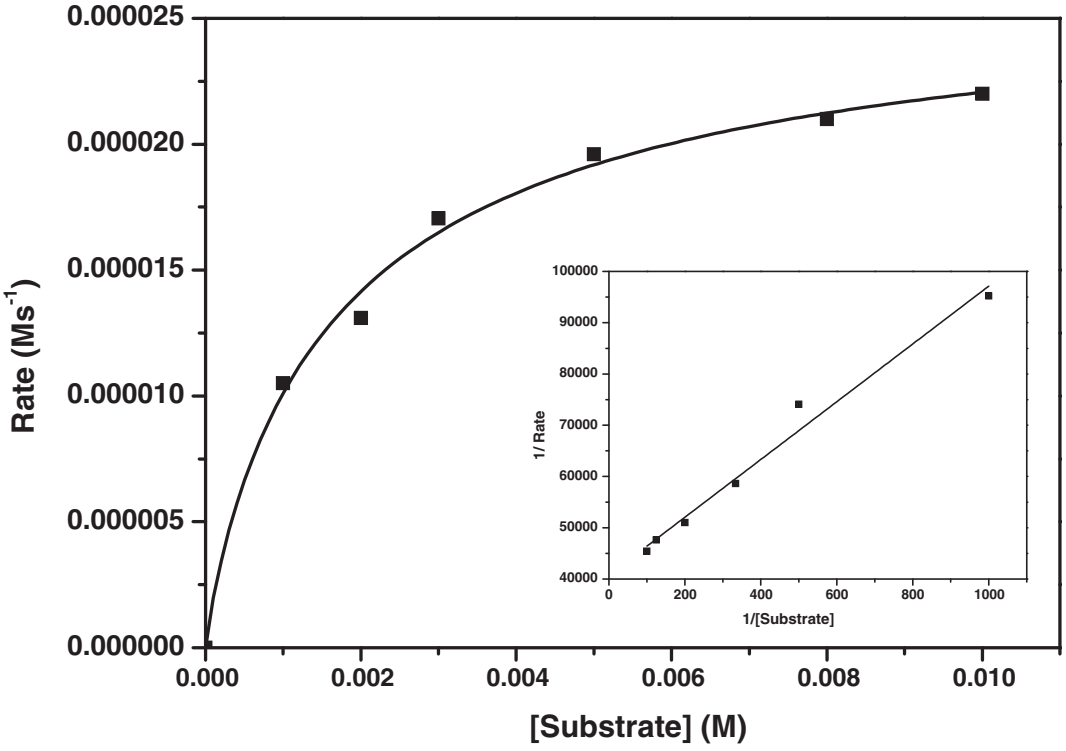


**Figure 4.** Plot of rate *vs.* [substrate] in presence of $[\mathbf{1}]^+$ in MeOH; inset: Lineweaver-Burk plot.

**Table 2.** Kinetic parameters for the oxidation of 3,5-DTBC catalyzed by $[\mathbf{1}]^+$ in methanol.

| Complex | Solvent | $V_{max}$ (M $s^{-1}$) | $K_m$(M) | $K_{cat}(h^{-1})$ | Reference |
|---|---|---|---|---|---|
| *$[\mathbf{1}]^+$ | MeOH | $2.68\times10^{-5}$ | $1.77\times10^{-3}$ | $9.65\times10^{2}$ | This paper |
| **1** | MeOH | $1.891\times10^{-5}$ | $1.57\times10^{-5}$ | $4.53\times10^{1}$ | 32 |
| **1** | MeOH | $3.36\times10^{-5}$ | $7.38\times10^{-4}$ | $1.21\times10^{3}$ | 33 |
| **1** | MeCN | $1.33\times10^{-5}$ | $8.70\times10^{-3}$ | $7.97\times10^{1}$ | 34 |
| **1** | MeOH | $7.23\times10^{-2}$ | $3.01\times10^{-6}$ | $4.82\times10^{2}$ | 32 |
| **1** | MeOH | $7.23\times10^{-2}$ | $7.23\times10^{-2}$ | $4.29\times10^{-2}$ | 35 |

*Std. Error for $V_{max}$ ($MS^{-1}$) $= 4.11\times10^{-6}$; Std. Error for $K_m$(M)$= 6.62\times10^{-4}$

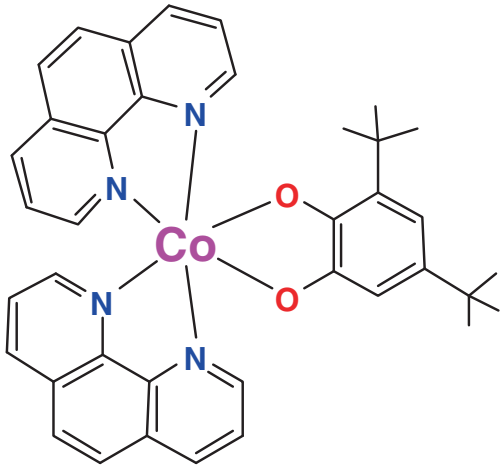


**Scheme 3.** Formation of mononuclear intermediate species during the course of catechol oxidation.

The ability of $[\mathbf{1}]^+$ to cleave DNA was assayed with the aid of gel electrophoresis on pBR 322 DNA as the substrate in a medium of 5 mM Tris–HCl/50 mM NaCl buffer (pH 7.1) in the absence of external additives. The DNA was mixed with different concentrations (25, 50, 75 and 100 $\mu$g) of Co(III) complex and was incubated at 37°C for 1 h. Figure 5 reveals the cleavage activity of $[\mathbf{1}]^+$ on pBR 322 DNA. Lane 1 shows the pBR 322 DNA control. Lane 2 shows the DNA treated with 25 $\mu$g of complex $[\mathbf{1}]^+$. There was a partial cleavage of the DNA with the addition of 25 $\mu$g of the complex. Further addition of different concentrations (50, 75 and 100 $\mu$g) of the complex in Lane 3, Lane 4, and Lane 5 did not show bands for the DNA. This finding clearly suggests that the concentration of the complex needed to cleave the pBR 322 DNA was 50 $\mu$g.

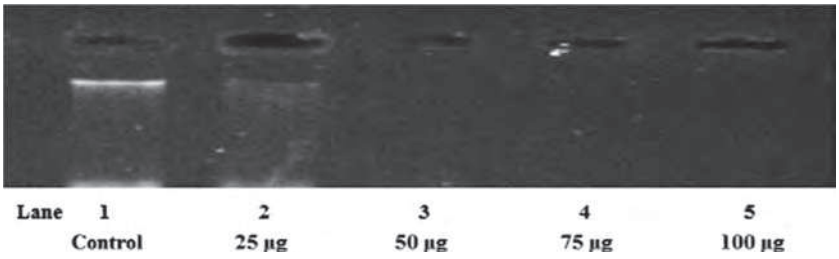


**Figure 5.** Concentration-dependent cleavage of plasmid pBR 322 DNA by $[\mathbf{1}]^+$ . Lane 1 shows the control DNA. Lane 2 shows DNA + sample (25 $\mu$g); lane 3, DNA+ sample (50 $\mu$g); lane 4, (75 $\mu$g); lane 5, (100 $\mu$g).

**Table 3.** UV Spectroscopic readings of pBR 322 DNA with $[\mathbf{1}]^+$.

| Sample | Absorbance at 260 nm | Concentration of DNA |
|---|---|---|
| Control pBR 322 DNA | 2.4 | 6 $\mu$g/mL |
| pBR 322 DNA + 25 $\mu$g $[\mathbf{1}]^+$ | 1.39 | 3.4 $\mu$g/mL |
| pBR 322 DNA + 50 $\mu$g $[\mathbf{1}]^+$ | 0.65 | 1.62 $\mu$g/mL |
| pBR 322 DNA + 75 $\mu$g $[\mathbf{1}]^+$ | 0.32 | 0.80 $\mu$g/mL |
| pBR 322 DNA + 100 $\mu$g $[\mathbf{1}]^+$ | 0.15 | 0.3 $\mu$g/mL |

To confirm the cleavage activity of $[\mathbf{1}]^+$ on the DNA, UV spectroscopic analysis was performed for the control pBR 322 DNA and DNA with different concentrations of the complex (Table 3). The concentration of the DNA showed a gradual decrease with increasing concentrations of the complex (Figure S6). The concentration of DNA sample can be checked by the use of UV spectrophotometry. DNA absorbs UV light very efficiently which makes it possible to detect and quantify at a concentration as low as 2.5 ng/$\mu$L. The nitrogenous bases in nucleotides have an absorption maximum at about 260 nm. The DNA concentration was calculated using the formula, DNA concentration ($\mu$g/mL) = (OD 260) × (dilution factor) × (50 $\mu$g DNA/mL)/(1 OD260 unit). The control had 6 $\mu$g/mL of DNA. There was a gradual decrease in the concentration of the DNA when added with increasing concentrations of $[\mathbf{1}]^+$ complex. This clearly shows that the complex played a major role in cleavage of pBR 322 DNA.

### 3.7 *Anti-cancer activity of the [1]$^+$ complex*

It is now well accepted that metal coordination compounds with metal–ligand exchange rates comparable to cell-division processes, often appear to be highly active as anti-cancer agents.[38b] A all third generation drugs (*vide supra*) appear to bind to a guanine-N7 site and this binding seems to be essential for the effect induced in DNA. Different compounds, however, appear to have different binding kinetics, and also the structural details of the resulting DNA adducts appear to differ to some degree.[38c] The anti-cancer activity associated with $[\mathbf{1}]^+$ is also associated with the presence of two fairly labile cis ligands and two phenanthroline ligands that are inert to substitution under biological conditions.

3.7a *3-(4,5-dimethylthiazol-2-yl)-2,5-diphenyltetrazolium bromide (MTT) Assay*: The present $[Co(phen)_2Cl_2]^+$, $[\mathbf{1}]^+$ complex has the ability to strongly bind and cleave DNA in the absence of an external agent and DNA cleavage is considered as an important step for a drug to act as an anti-cancer agent.[38–40] Thus, the cytotoxicity of the $[\mathbf{1}]^+$ dissolved in DMSO was investigated against a human hepatocarcinoma cell line (HepG2) adopting MTT assay. The $IC_{50}$ values of $[\mathbf{1}]^+$ were obtained by plotting the cell viability against the concentration of the complex (Figure S7). The results revealed that the $IC_{50}$ at 48 h (170± 0.2 $\mu$M) is lower than that at 24 h (175± 0.3 $\mu$M) clearly indicating that the complex exhibits cytotoxicity against HepG2 in dose- and duration-dependent manner. Thus, the cytotoxicity exhibited by the complex is consistent with its strong binding with DNA, and its efficiency in cleaving DNA in the absence of an external agent is responsible for its potency to induce cell death through different modes of interaction between the cationic complex and DNA.

3.7b *AO/EB staining*: Apoptotic cell death is known as characterized by different cellular changes such as

cell shrinkage, nuclear condensation, DNA fragmentation, membrane blebbing and formation of apoptotic bodies. These apoptotic characteristics as produced in human hepatocarcinoma cell (HepG2) by $[\mathbf{1}]^+$ were analyzed adopting AO/EB staining. In this staining method, the fluorescence pattern depends on the viability and membrane integrity of the cells. In general, dead cells are permeable to ethidium bromide and fluoresce in orange-red, whereas live cells are permeable to acridine orange only and thus fluoresce in green. The cytological changes which were observed in the treated cells are classified into four types based on the fluorescence emission and morphological features of chromatin condensation in the AO/EB stained nuclei: i) Viable cells, which are having highly organized nuclei, fluoresce in green. ii) Early apoptotic cells, which show nuclear condensation, emit orange-green fluorescence. iii) Late apoptotic cells, with highly condensed or fragmented chromatin, fluoresce orange to red. iv) Necrotic cells fluoresce orange to red, with no indication of chromatin fragmentation. All these morphological changes were observed after the treatment of cancer cells with the complex. Figure 6 indicates the apoptotic morphologies induced by $[\mathbf{1}]^+$ at $IC_{50}$ concentration for 24 h. The cobalt(III) complex, $[\mathbf{1}]^+$ being a cationic molecule with two chlorine atoms at *cis* position (<Cl-Co-Cl = 92°) and labile groups at cisoid position around metal centres, is of considerable attraction in biology, specially as anticance agents.[41] The cisoid labiles groups facilitate the path of substitution of the labile groups by the nitrogenous base (purine and pyrimidine) of the DNA and the $[\mathbf{1}]^+$-DNA adduct enhances distortion in DNA molecules which causes apoptosis of the affected cells. On the other hand, $[Co(phen)_2Cl_2]^+$ has two phenanthroline ligands which can intercalate into nitrogenous base pairs and elongate the DNA to some extent. Intercalative binding can also kill the affected DNA molecules. Figure 7 shows the efficacy of $[\mathbf{1}]^+$ to induce apoptosis in 53% of cells when treated for 24 hr and there is no indication of necrotic cell death compared to untreated controls. The $IC_{50}$ values and morphological changes consolidate the potential anticancer activity of the molecule. However, further studies are needed in this direction to decipher the molecular mechanisms underlying the mode of cell death induced by $[\mathbf{1}]^+$.

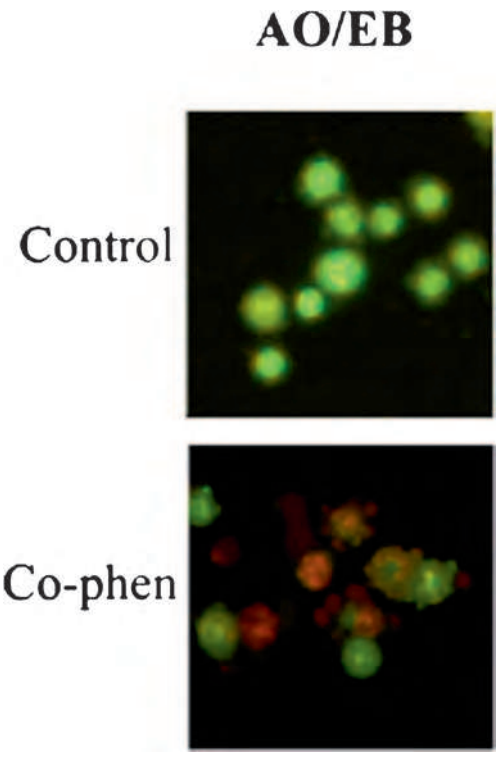


**Figure 6.** Representative morphological changes observed for $[\mathbf{1}]^+$ with AO/EB staining against HepG2 cells at 24 h incubation.

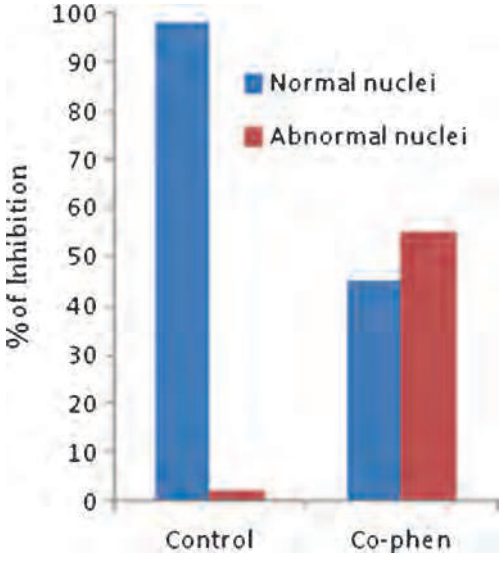


**Figure 7.** The effect of $[\mathbf{1}]^+$ on HepG2 cell as revealed in acridine orange and ethidium bromide staining. Relative percentage of morphological changes was determined and classified into three categories: viable, apoptosis and necrosis as compared with the control cells after 24 h incubation.

3.7c *Hoechst Staining*: Morphological changes in the nucleus and chromatin were revealed by Hoechst 33528 staining method. The cells treated with $IC_{50}$ concentration of the complex showed some changes in their morphology of nuclei compared to the control untreated nuclei. In the untreated control cells the nuclei were round with intact chromatin while after treatment with the complex for 24 h changes such as chromatin marginalization, condensation and fragmentation were

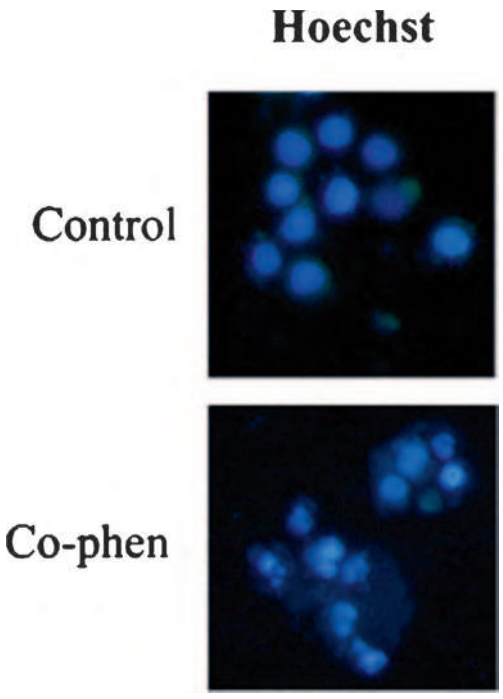


**Figure 8.** Representative morphological changes observed for $[\mathbf{1}]^+$ with Hoechst 33258 staining against HepG2 at 24 h incubation.

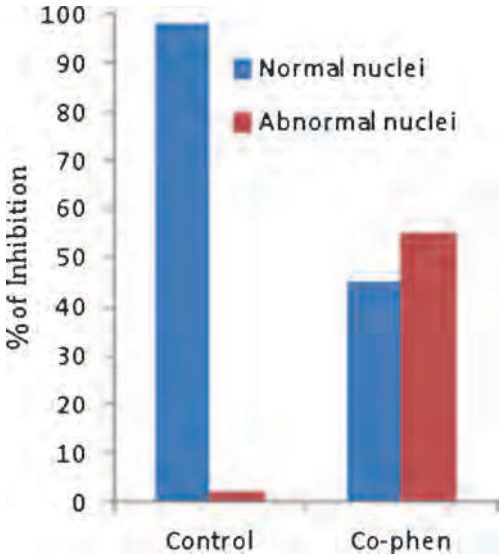


**Figure 9.** The effect of $[\mathbf{1}]^+$ on HepG2 cell as revealed in Hoechst staining. Relative percentage of morphological changes was determined and classified into two categories: normal and abnormal nuclei as compared with the control cells after 24 h incubation.

observed. Figure 8 indicates the apoptotic nuclear morphology induced at $IC_{50}$ concentration by the complex for 24 h. It is interesting that 55% of treated cells exhibited abnormal nuclei (Figure 9).

### 3.8 *Thermogravimetric analysis*

The thermal behaviour of the complexes $[\mathbf{1}]NO_3{\cdot}3H_2O$ and $[\mathbf{1}]NO_3{\cdot}CH_3CO_2H{\cdot}H_2O$ were followed up to 700°C in a static nitrogen atmosphere with a heating rate of 10°C per minute. Thermal analysis of $[\mathbf{1}]NO_3{\cdot}3H_2O$ shows that the loss in the temperature range 100–197°C is 6.15% (figure S8), corresponding to two water molecules. The loss of total solvent molecules (16.1%) at higher temperature (100–275°C) is attributed to the strong interaction of the water-nitrate anions. The release of two coordinated chlorine atoms takes place in the second step (275.48–316.80°C). The experimental mass loss 19.081% agrees well with the calculated mass loss 14.55%. The residual part of the phenanthroline moieties takes place in the last step.

In the case of $[\mathbf{1}]NO_3{\cdot}CH_3CO_2H{\cdot}H_2O$, there is continuous loss of solvent that starts at about 40°C and the release of acetic acid-water-nitrate occurs up to 289°C (Figure S9). The next step between 289.81°C and 425.08°C corresponds with the loss of two coordinated chlorine atoms and the residual part of the phenanthroline moieties take place in the last step (425.08–626.51°C).

## 4. Conclusions

We have synthesized and crystallographically characterized two mononuclear *cis*-Co(III)-phenanthroline compounds. The cationic cobalt(III) complexex, $[\mathbf{1}]^+$ exhibits very efficient catalytic activity in saturated oxygen environment towards *3,5-ditert*butylcatechol with $k_{cat}$ value $9.65\times10^2$ $h^{-1}$. $[\mathbf{1}]^+$ is one of the few examples of mononuclear cobalt(III) complexes containing catalyst of catecholase activity for which both the single crystal X-ray structure and $K_{cat}$ value have been determined. Besides, $[\mathbf{1}]^+$ being a mononuclear cobalt(III) complex with non-copper centre is mimicking an enzyme with a dicopper active site. $[\mathbf{1}]^+$ induces very efficient cleavage of double-stranded DNA without the requirement of activating agents and exhibits important cytotoxicity against human hepatocarcinoma cell line (HepG2) in terms of damaging the DNA in cancer cells. Moreover, detailed experimentation related to DNA interaction, cleavage and cytotoxicity on this complex will help to develop clinically relevant information for possible new anticancer agents.

## Supplementary Information

Crystallographic data are available free of charge from The Director, CCDC, 12 Union Road, Cambridge, CB2 1EZ, UK (fax: +44-1223-336033;

E-mail: deposit@ccdc.cam.ac.uk or www: http://www.ccdc.cam.ac.uk) upon request, quoting deposition number CCDC 829003 for [**1**]$NO_3 \cdot 3H_2O$ and and CCDC 975400 for [**1**]$NO_3 \cdot CH_3CO_2H \cdot H_2O$. Figures S1-S9 and tables S1-S3 are available in the online version at www.ias.ac.in/chemsci.

**Acknowledgements**

The work was supported financially by the Department of Science and Technology (DST), New Delhi, India under FAST TRACK SCHEME for YOUNG SCIENTIST (NO. SB/FT/CS-088/2013 dtd. 21/05/2014). B. Biswas also gratefully acknowledges the financial support from the University Grant Commission, New Delhi, India (F. No. PSW-84/12-13(ERO) dated 05/02/2013). B. Biswas is highly thankful to IACS, Kolkata for facilitating proton NMR and mass spectrometric studies.

**References**

1. (a) Long E C and Barton J K 1990 *Acc. Chem. Res.* **23** 271; (b) Selvi P T, Evans H S, Palaniandavar M 2005 *J. Inorg. Biochem.* **99** 2110
2. (a) Sammes P G and Yahioglu G 1994 *Chem. Soc. Rev.* **23** 327; (b) Shields T P, Barton J K, 1995 *Biochemistry* **34** 15037; (c) Vaidyanathan V G, Nair B U 2003 *J. Inorg. Biochem.* **94** 121
3. (a) Barton J K and Raphael A L 1984 *J. Am. Chem. Soc.* **106** 2466; (b) Wang X L, Chao H, Li H, Hong X L, Liu Y J, Tan L F and Ji L N 2004 *J. Inorg. Biochem.* **98** 1143
4. (a) Sitlani A S, Long E C, Pyle A M, Barton J K 1992 *J. Am. Chem. Soc.* **114** 2303; (b) Dey D, Pal S, Chandraleka S, Dhanasekaran D, Kole N and Biswas B 2014 *J. Indian Chem. Soc.* **91** 1267
5. (a) Chan S and Wong W T 1995 *Coord. Chem. Rev.* **138** 219; (b) Zhen Q-X, Ye B-H, Zhang Q-L, Liu J-G, Li H, Ji L-N and Wang L 1999 *J. Inorg. Biochem.* **76** 47; (c) Dey D, Kaur G, Ranjani A, Gyathri L, Chakraborty P, Adhikary J, Pasan J, Dhanasekaran D, Choudhury A R, Akbarsha M A, Kole N and Biswas B 2014 *Eur. J. Inorg. Chem.* 3350
6. (a) Pratviel G, Bernadou J and Meunier B 1998 *Adv. Inorg. Chem.* **45** 251; (b) Shimakoshi H, Kaieda T, Matsuo T, Sato H and Hisaeda Y 2003 *Tetrahedron Lett.* **44** 5197; (c) Biswas B, Mitra P and Ghosh R 2013 *J. Indian Chem. Soc.* **90** 1311
7. (a) Liang F, Wang P, Zhou X, Li T, Li Z Y, Lin H K, Gao D Z, Zheng C Y and Wu CT 2004 *Bioorg. Med. Chem. Lett.* **14** 1901; (b) Biswas B, Mitra M, Pal A, Basu A, Rajalakshmi S, Mitra P, Aliaga-Alcalde N, Kumar G S, Nair B U and Ghosh R 2013 *Ind. J. Chem. Sect. A* **52A** 1576
8. (a) Biswas B, Patra M, Dutta S, Ganguly M and Kole N 2013 *J. Chem. Sci.* **125** 1445; (b) Pal A, Biswas B, Mondal S K, Lin C-H and Ghosh R 2012 *Polyhedron* **31** 671
9. (a) Parshall G and Ittel S (Eds.)1992 *Homogeneous Catalysis* 2nd edition (New York: John Wiley); (b) Biswas B, Al-Hunaiti A, Räisänen M T, Ansalone S, Leskelä M, Repo T, Chen Y-T, Tsai H-L, Naik A D, Railliet A P, Garcia Y, Ghosh R and Kole N 2012 *Eur. J. Inorg. Chem.* 4479
10. Cornils B and Herrmann W (Eds.) 1996 *Applied Homogeneous Catalysis with Organometallic Compounds* Vol. 1 (Weinheim: VCH)
11. Anastas P and Warner J 1997 In *Green Chemistry: Theory and Practice* (Oxford: Oxford University Press)
12. (a) Puzari A and Jubaraj B 2002 *J. Mol. Cat. A Chem.* **187** 149; (b) Biswas B, Mitra M, Adhikary J, Krishna G R, Bag P P, Reddy C M, Aliaga-Alcalde N, Chattopadhyay T, Das D and Ghosh R 2013 *Polyhedron* **53** 264
13. (a) Gates B 1992 In *Catalytic Chemistry* (Hoboken: John Wiley); (b) Dey D, Kaur G, Patra M, Choudhury A R, Kole N and Biswas B 2014 *Inorg. Chim. Acta* **421** 335
14. Foote C, Valentine J, Greenberg A and Liebman J 1995 In *Active Oxygen in Chemistry*, SEARCH Series, Vol. 2 (Kluver)
15. (a) Mayer A M and Harel E 1979 *Phytochem* **18** 193; (b) Simándi T L and Simándi L I 1998 *React Kinet. Catal. Lett.* **65** 301; (c) Simándi L I and Simándi T L 1998 *J. Chem. Soc. Dalton Trans.* 3275; (d) Biswas A, Das L K and Ghosh A 2013 *Polyhedron* **61** 253
16. (a) Selmeczi K, Reglier M, Giorgi M and Speier G 2003 *Coord. Chem. Rev.* **245** 191; (b) Gerdemann C, Eicken C, Krebs B 2002 *Acc. Chem. Res.* **35** 183; (c) Guha A, Chattopadhyay T, Paul N D, Mukherjee M, Goswami S, Mondal TK, Zangrando E and Das D 2012 *Inorg. Chem.* **51** 8750
17. (a) Than R, Feldmann A A and Krebs B 1999 *Coord. Chem. Rev.* **182** 211; (d) Solomon E I, Sundaram U M, Machonkin T E 1996 *Chem. Rev.* **96** 2563; (f) Klabunde T, Eicken C, Sacchettini J C and Krebs B 1998 *Nat. Struct. Biol.* **5** 1084; (g) C Eicken, Krebs B and Sacchettini J C 1999 *Curr. Opin. Struct. Biol.* **9** 677
18. (a) Dervall B J 1961 *Nature* **189** 311; (b) Koval I A, Gamez P, Belle C, Selmeczi K, Reedijk J 2006 *Chem. Soc. Rev.* **35** 814; (c) Kitajima N and Moro-oka Y 1994 *Chem. Rev.* **94** 737
19. Youssef NS El-Zahany E, El-Seidy A M A, Caselli A and Cenini S 2009 *J. Mol. Cat. A* **308** 159
20. (a) Chan T L, To C T, Liao B-S, Liu S-T and Chan K S 2012 *Eur. J. Inorg. Chem.* 485; (b) Arzberger S, Soper J, Anderson O P, la Cour A and Wicholas M 1999 *Inorg. Chem.* **38** 757
21. (a) Simandi L I, Barna T, Argay G and Simandi T L 1995 *Inorg. Chem.* **34** 6337; (b) Chakrabarty R, Sarmah P, Saha B, Chakravorty S and Das B K 2009 *Inorg. Chem.* **48** 6371
22. Ghosh S, Barve A C, Kumbhar A A, Kumbhar A S, Puranik V G, Datar P A, Sonawane U B and Joshi R R 2006 *J. Inorg. Biochem.* **100** 331
23. SHELXTL 5.10 Bruker Analytical X−ray Instruments Inc.,Karlsruche, Germany (1997)

24. Farrugia L J, ORTEP-32 for Windows, University of Glasgow, Scotland (1998)
25. Mosmann T 1983 *J. Immun. Met.* **65** 55
26. Spector D L, Goldman R D and Leinwand L A 1998 In *Cell: A Laboratory Manual. Culture and Biochemical Analysis of Cells* Vol. 1 (New York: Cold Spring Harbor Laboratory Press)
27. Nakamoto K 1997 In *Infrared and Raman Spectra of Inorganic and Coordination Compounds part B: Applications in Coordination, Organometallic and Bioinorganic Chemistry* (New York: John Wiley) p. 116
28. Sole J G, Bausa L E and Jaque D 2005 In *An Introduction to Optical Spectroscopy of Inorganic Solids* (John Wiley)
29. Tsuruya S, Yanai S-I and Masai M 1986 *Inorg. Chem.* **25** 141
30. Zippel F, Ahlers F, Werner R, Haase W, Nolting H-F and Krebs B 1996 *Inorg. Chem.* **35** 3409
31. Banu K S, Chattopadhyay T, Banerjee A, Mukherjee M, Bhattacharya S, Patra G K, Zangrando E and Das D 2009 *Dalton Trans.* 8755
32. Majumder S, Mondal S, Lemoineb P and Mohanta S 2013 *Dalton Trans.* **42** 4561
33. Ghosh R, Mitra M and Raghavaiah P 2015 *New J. Chem.* **39** 200
34. Dey S K and Mukherjee A 2014 *New J. Chem*. **38** 4985
35. Banerjee A, Guha A, Adhikary J, Khan A, Manna K, Dey S, Zangrando E and Das D 2013 *Polyhedron* **60** 102
36. Vaidyanathan V G and Nair B U 2003 *J. Inorg. Biochem.* **94** 121
37. (a) Liu X W, Li J, Li H, Zheng K C, Chao H and Ji L N 2006 *J Inorg Biochem* **100** 385; (b) Chao H, Mei W J, Huang Q W and Ji L N 2002 *J Inorg Biochem* **92** 165
38. (a) Basile L A, Raphael A L and Barton J K 1987 *J. Am. Chem. Soc.* **109** 7550; (b) Hartwig J F and Lippard S J 1992 *J. Am. Chem. Soc.* **114** 5646; (c) Reedijk J 2009 *Eur. J. Inorg. Chem.* 1303
39. (a) Ramakrishnan S, Suresh E, Riyasdeen A, Periasamy V S, Akbarsha M A, Palaniandavar M 2011 *Dalton Trans.* **40** 3245; (b) Satyanaryana S, Dabrowiak J C and Chaires J B 1993 *Biochemistry* **32** 2573; (c) Wang X 2010 *Anticancer Agents Med. Chem.* **10** 396
40. (a) Wang X and Guo Z 2013 *Chem. Soc. Rev.* **42** 202; (b) Tabassum S, Parveen S and Arjmand F 2005 *Acta Biomater.* **1** 677; (c) Pasternack R F, Gibbs E J and Villafranca J J 1983 *Biochemistry* **22** 2406
41. (a) Hannon M J 2007 *Pure Appl. Chem.* **79** 2243; (b) Oberoi H S, Nukolova N V, Kabanov A V and Bronich T K 2013 *Adv. Drug Delivery Rev.* **65** 1667